Development of $POCl_3$ emitters which enable Ag reduction while increasing solar cell efficiency: Assessing the impact on manufacturing and system costs

Ian B. Cooper[1], **Keith Tate**[1], **Moon Hee Kang**[1], **Alan F. Carroll**[2], **Kurt R. Mikeska**[3], **Robert C. Reedy**[4] & **Ajeet Rohatgi**[1]
[1]University Center of Excellence for Photovoltaics Research and Education, Georgia Institute of Technology, Atlanta; [2]DuPont Microcircuit Materials, Research Triangle Park, North Carolina; [3]DuPont Central Research & Development, Wilmington, Delaware; [4]National Renewable Energy Laboratory, Golden, Colorado, USA

ABSTRACT

The market price of Ag has fluctuated considerably over the past ten years and has impacted the manufacturing cost of Si solar cells and the price of Si PV. Reducing Ag consumption can decrease this cost; however, such reduction may come at the expense of cell performance. In order to address the issue of Ag cost reduction while maintaining high cell efficiency, phosphorus emitter profiles are tailored via $POCl_3$ diffusion to create solar cell emitters displaying low saturation current density (J_{0e}), variable electrically active surface phosphorus concentration ([$P_{surface}$]), and variable sheet resistance with the aim of reducing Ag consumption. By optimizing emitter diffusion conditions, it is possible to reduce screen-printed Ag paste consumption by 33% with no loss in cell performance. Using a screen-printable Ag conductor paste designed to contact low [$P_{surface}$] emitters, the performance of cells with screen-printed Ag paste dry masses of 200, 120 and 80mg is compared. By using a tailored low-J_{0e} 55Ω/sq emitter, it is possible to achieve a high open-circuit voltage (V_{oc}) and short-circuit current (J_{sc}) to yield average cell efficiencies of 18.64% and 18.73% for 120mg and 80mg Ag paste dry mass, respectively. This is compared with efficiencies of 18.52% for cells using state-of-the-art technology (industrial high [$P_{surface}$] 65Ω/sq emitter with 120mg Ag paste dry mass). On the basis of a Ag market price of US$32/troy oz and an 85% by weight thick-film paste Ag metal content, a Ag front-side metallization cost of US¢2.11/W can be achieved by using 80mg Ag paste dry mass, which translates to a Ag cost saving of US$5.4M per year for a 500MW production line when compared with the Ag cost for state-of-the-art technology. Further cost analysis shows a 1.2% area-related balance of system (BOS) cost reduction and a US¢0.1/kWh reduction when comparing low-J_{0e} 55Ω/sq modules and state-of-the-art modules. Calculations show that an additional 0.5% absolute efficiency for state-of-the-art modules is required, to compensate the efficiency gains and Ag cost reduction afforded by low-J_{0e} 55Ω/sq modules.

Introduction

For the PV industry to attain grid parity and reach a place of sustainability, installed system efficiency must increase while installed system cost must decrease. The US Department of Energy has mandated significant cost reductions in order for PV to become and remain cost-competitive with traditional energy sources [1]. In addition to streamlining BOS costs and soft costs associated with electrical permitting and consumer financing, module- and cell-level improvements will impact the efficiency and cost of the final system. Numerous organizations have published cell-level improvements indicating the potential for high efficiency. However, many improvements come with additional processing steps and materials which, because of added capital expense, tend to negate potential gains.

Figure 1. Market price of Ag from January 1975 to August 2012 in US$ per troy oz. Lowest price was $3.56/oz in March 1993; highest prices were $49.45/oz in January 1980 and $48.70/oz in April 2011 [2].

> "Contact metallization is one of the most expensive parts of Si solar cell fabrication."

Contact metallization is one of the most expensive steps in Si solar cell fabrication, since a majority of cells receive screen-printed thick-film Ag for the front-side collection grid. Over the past 40 years (see Fig. 1 [2]), the market price of Ag has seen dramatic shifts due to events like the Hunt brothers market-cornering scandal of 1980, as well as recent interest in Ag as an investment tool and the emergence of

Ag exchange-traded funds (ETFs) [3]. In the last ten years alone, the market price of Ag has fluctuated between $5 and $49 per troy ounce, ultimately impacting the manufacturing cost of Si solar cells and the price of c-Si PV. Although Ag price has fallen from its recent peak in April 2011, in order to reduce the cost of solar electricity generated by c-Si PV, the amount of Ag per cell needs to be reduced. The International Technology Roadmap for Photovoltaics (ITRPV) predicts that Ag consumption at the cell level will fall to 50mg by 2017 with the assumption that a transformative, manufacturable Cu-based metallization technology will be implemented by 2015 [4]. However, since Ag is the primary conductor involved in minority-carrier collection, simply reducing Ag consumption may result in the loss of cell performance due to degradation of fill factor (*FF*) and increased series resistance (R_{series}). Much effort has gone into research and development of metallization alternatives to Ag, such as Ni plating for the formation of Ni silicide contacts [5–6] as well as Cu plating and screen printing [7–11].

In addition to costs being lowered through a reduction in material consumption, solar cell performance must continue to rise in parallel. One potential route to achieving high efficiency is the use of lightly doped, low [$P_{surface}$] n^+ emitters on p-type wafers. Lightly doped emitters are recognized for the potential for higher V_{oc} and J_{sc}, through lower J_{0e} and higher short-wavelength response, respectively [12]. Low [$P_{surface}$] emitters have been studied and produced by novel methods [13,14]; however, contacting such emitters with conventional screen-printed thick-film Ag pastes is challenging and leads to very high Ag/Si contact resistance and high R_{series}. Poor contact to lightly doped emitters using thick-film Ag pastes is most likely due to the insufficient formation of current-transport structures/pathways at the Ag/Si contact interface and/or the formation of insulating interfacial glass layers, both of which prevent an efficient transfer of minority carriers from the bulk Si to the Ag collection grid.

Recently, using standard $POCl_3$ diffusion processes, Cooper et al. [15] demonstrated homogeneous n^+ emitters showing low J_{0e} and low [$P_{surface}$] that displayed low contact resistance using a screen-printable Ag conductor paste [16] specifically tailored to contact low [$P_{surface}$] emitters. Low-milliohm Ag/Si-specific contact resistance values were observed for solar cells with emitter active [$P_{surface}$] as low as 9E19cm^{-3}, and final V_{oc} values as high as 637mV were achieved on a relatively low emitter sheet resistance of 65Ω/sq.

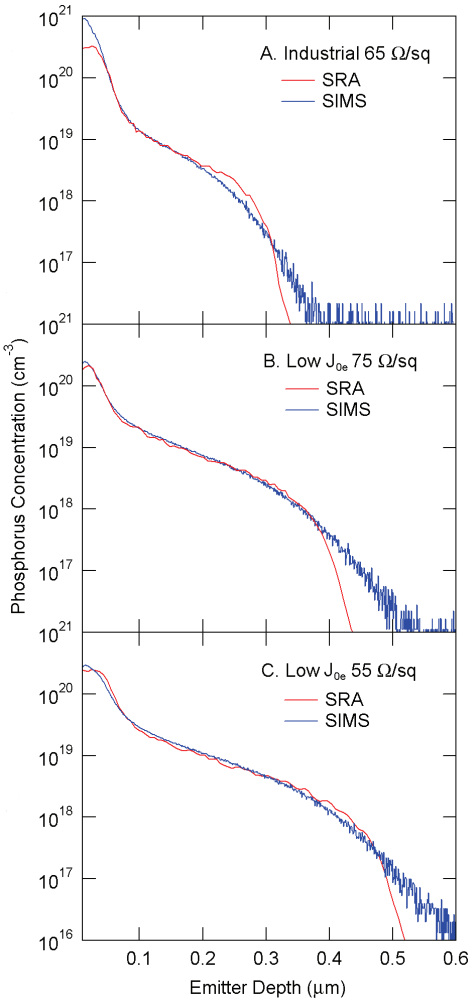

Figure 2. Spreading resistance (SRA) and secondary ion mass spectrometry (SIMS) profiles for: (A) industrial 65Ω/sq; (B) low-J_{0e} 75Ω/sq; and (C) low-J_{0e} 55Ω/sq emitters.

> "To address the problem of excess Ag consumption, the emitter sheet resistance is reduced while maintaining high emitter quality."

To address the problem of excess Ag consumption, contrary to conventional wisdom, the emitter sheet resistance is reduced while maintaining high emitter quality, as indicated by J_{0e}, implied V_{oc} and final V_{oc} measurements. The reduction in sheet resistance allows lower gridline pitch for the standard three-busbar H pattern (65 gridlines reduced to 50 gridlines). The reduction in gridline pitch in combination with narrower gridlines (>100µm reduced to 75–85µm) results in ~0.2% higher average cell efficiencies while decreasing Ag consumption by 33% as compared with the industry state of the art. Using the average solar cell efficiency/paste mass combinations presented, we speculate on what impact such a Ag reduction and an efficiency increase will have on system costs.

Cell fabrication and characterization

Large area (239cm^2) n^+-p-p^+ Si solar cells were fabricated on 1–3Ωcm B-doped Cz Si wafers of thickness 180–200µm. All wafers were anisotropically textured via KOH/isopropanol solution to attain quadrilateral pyramid size in the range of 3 to 7µm. n^+-p junctions were formed by $POCl_3$ tube diffusion in a Centrotherm furnace. Emitter sheet resistance and diffusion profile were manipulated by varying the time, temperature, $POCl_3$ bubbler N_2 flow rate, and O_2 flow rate of the furnace during diffusion. Following chemical edge isolation and phosphosilicate glass (PSG) removal, emitters were sunny-side coated with a SiN_x anti-reflective coating using a Centrotherm PECVD reactor. All wafers were screen printed via a semi-automated ASYS printer with DuPont Solamet PV17F to form the three-busbar H grid patterns. Ag screen printing was controlled to deliver 200 and 120mg dry paste mass, forming 65 gridlines, and 80mg dry paste mass, forming 50 gridlines. Commercially

Saving you up to 35% in capital costs isn't a claim BTU makes lightly. But as they say, "the proof is in the throughputting."

BTU's amazing Tritan™, with its revolutionary TriSpeed technology, brings dual-lane firing to the next level. Expect bar-raising performance, with superior ramp rates, and increased cell efficiency.

But don't take our word for it. Send us your wafers and demand proof. In a bottom-line world, that's promising.

Tritan™
Metallization Firing Furnace

BTU

we PROMISE more PROFITS with PROOF

www.BTU.com

Pioneering Products and Process Solutions for
In-Line Diffusion • Metallization • Thin Film

Let us prove our claims!

available Al and Ag/Al pastes were screen printed on the rear side of all wafers for the formation of an Al back-surface field (Al-BSF) and rear tabbing stripes, respectively. After each screen-printing event, wafers were dried at 175°C in an IR belt furnace for one minute and fired in a seven-zone IR belt furnace from TPSolar.

A Sinton WCT-120 Photoconductance Lifetime Tester was used to estimate J_{0e} and implied V_{oc} for each emitter via quasi-steady state photoconductance decay (QSSPCD). Representative samples for J_{0e} and implied V_{oc} measurement were SiN_x coated on both sides after PSG removal and subjected to simulated contact firing. J_{0e} and implied V_{oc} values are reported at one-sun illumination (1.6–6.7E14 carriers/cm^2 injection level). J_{0e} is calculated from total J_0 ($J_0 = J_{sc}/e^{(imp\ Voc \cdot q/k \cdot T)}$, where J_{sc} = 37.3mA/cm^2) by subtracting the bulk contribution ($J_{0b} = qn_i^2W/N_A\tau_{bulk}$, where q is the fundamental charge, n_i is the intrinsic carrier concentration, W is the wafer thickness, N_A is the base dopant concentration, and τ_{bulk} is the minority carrier lifetime of the wafer) and dividing the result by two since J_{0e} samples are two-sided symmetric structures [17]. Emitter doping profiles were measured via spreading resistance analysis (SRA) by Solecon Laboratories, Inc., and by secondary ion mass spectrometry (SIMS) at the National Renewable Energy Laboratory. Profile wafers were mirror polished and of a light base doping (15–20Ωcm resistivity) to allow [$P_{surface}$] and n$^+$-p metallurgical junction depth to be accurately established. Profile wafers were diffused in the centre of a full Cz wafer diffusion to simulate tube-packing conditions.

Comparison of industry state-of-the-art and low-J_{0e} emitters and solar cells

A series of n$^+$ emitters displaying low J_{0e} and variable [$P_{surface}$] were recently introduced in order to study the limits of low-resistance Ag thick-film contact [15]. In an extension of that study, the $POCl_3$ diffusion parameters were further refined, to create emitters with low [$P_{surface}$] and low J_{0e} while keeping sheet resistance low. Starting from diffusion conditions which resulted in a 75Ω/sq emitter with low J_{0e} and low [$P_{surface}$], the diffusion parameters were tuned to lower the sheet resistance to 55Ω/sq without a penalty in J_{0e}.

For comparison, this study includes a high [$P_{surface}$] 65Ω/sq emitter, which can be considered an industrial emitter easily contacted by most commercially available thick-film Ag pastes. Fig. 2 shows the dopant profiles for the industrial emitter (Fig. 2A) and two experimental emitters (Figs. 2B and 2C) used in the current study. Clear differences can be seen in [$P_{surface}$], in the depth of high [$P_{surface}$] near the wafer surface, and in the n$^+$-p junction depth when comparing industrial 65Ω/sq (Fig. 2A), low-J_{0e} 75Ω/sq (Fig. 2B) and low-J_{0e} 55Ω/sq (Fig. 2C) dopant profiles. In Fig. 2, electrically active [P] (red curve; SRA) and total [P] (blue curve; SIMS) are compared for each emitter. Samples for SRA and SIMS measurements were chipped from adjacent positions at the centre of profile wafers post-diffusion. A comparison of SRA and SIMS curves for the two experimental emitters reveals strong similarities as expected. However, the curves diverge sharply for the industrial 65Ω/sq emitter between 0 and 40nm depth. This divergence is accounted for by the substantial inactive P or 'dead layer' associated with the industrial emitter. Comparison of SRA and SIMS curves for the two experimental emitters show little or no inactive P.

Emitter	Active [$P_{surface}$] [atoms/cm^3]	n$^+$-p junction depth* [µm]	Implied V_{oc}** [mV]	J_{0e}** [fA/cm^2]
Industrial 65Ω/sq	3.5E20	0.33	631	394
Low J_{0e} 75Ω/sq	1.4E20	0.44	654	120
Low J_{0e} 55Ω/sq	2.5E20	0.52	652	149

* Based on device resistivity

** Implied V_{oc} and J_{0e} values derived from QSSPCD measurements

Table 1. Average physical and electrical characteristics of industrial and low-J_{0e} emitters.

Table 1 shows active [$P_{surface}$], n$^+$-p metallurgical junction depths based on device wafer resistivity, average implied V_{oc} and average J_{0e} for each emitter. Through emitter diffusion parameter tailoring, it was possible to achieve low J_{0e} and high implied V_{oc} values while decreasing emitter sheet resistance to 55Ω/sq, allowing flexibility in the Ag gridline pitch and total Ag consumption. The low J_{0e} value of 149fA/cm^2 observed for low-J_{0e} 55Ω/sq compared to 394fA/cm^2 for industrial 65Ω/sq is most likely due to the negligible inactive P layer found in low J_{0e} 55Ω/sq. A substantial 'dead layer', like that found in industrial 65Ω/sq, can lead to the formation of crystal defects and precipitates [17], thus degrading J_{0e}. Indeed, it is speculated that the decrease in precipitates associated with 'dead layer' elimination leads to a reduction in Shockley-Read-Hall recombination in the emitter, increased emitter minority-carrier lifetime, and improved surface passivation potential via applied dielectric layers [18].

It is possible to derive surface recombination velocities (SRV) associated with the emitters used in this study through internal quantum efficiency (IQE) curve fitting using PC1D solar cell modelling software [19]. Details for the specific PC1D input parameters used for SRV extraction can be found in Cooper et al. [15]. The short-wavelength region of solar cell IQE (300–600nm) is influenced by emitter quality. PC1D fitting of this region, with specific experimental external reflectance and SRA profile inputs for each emitter, produced SRV values of 1.2E5cm/s for industrial 65Ω/sq and 3.5E4cm/s for both low J_{0e} 75Ω/sq and low J_{0e} 55Ω/sq. In agreement with measured J_{0e} and implied V_{oc} values, a comparison of industrial 65Ω/sq with low J_{0e} 55Ω/sq reveals more than a factor of two difference in surface recombination, despite the similarity in sheet resistance.

Table 2 shows average light *I-V* performance for solar cells fabricated with the three emitters studied above and the three Ag paste dry masses used for front-side H grid pattern formation. Focusing first on the largest Ag paste mass (200mg), the average *FF* is greater than 0.79 for solar cells with each emitter. Previous specific contact resistance analysis of similar emitters showed contact resistance values ranging from 2 to 5mΩcm^2 using a similar Ag conductor paste [15]. Such low contact resistance combined with full gridlines provided by 200mg Ag paste mass enables low R_{series}.

As Ag paste mass decreased by reducing the Ag lay-down and number of gridlines, a higher solar cell J_{sc}, by up to 1mA/cm^2, is seen, but also *FF* is lower and R_{series} is higher (Table 2). The fall in *FF* and the rise in R_{series}, observed as the Ag paste dry mass decreases, arise from lower Ag gridline conductivity due to narrower gridlines and greater gridline pitch as a result of using 50 gridlines as opposed to 65. Because of the lower *FF* and higher R_{series}, cells made with industrial 65Ω/sq and low-J_{0e} 75Ω/sq emitters show a loss in efficiency, despite an increase in J_{sc}, when Ag paste dry mass is reduced to 80mg. However, the maximum efficiency observed for solar cells with a low-J_{0e} 55Ω/sq emitter occurs for the lowest Ag paste dry mass (80mg).

> "The true advantage of the low-J_{0e} emitters is the higher final V_{oc}."

It is important to note that the true advantage of the low-J_{0e} emitters is the higher final V_{oc}. Solar cells made with the

Emitter	Paste mass [mg] /gridline count	V_{oc} [mV]	J_{sc} [mA/cm^2]	*FF*	η[%]	*n* factor	R_{series} [Ωcm^2]	R_{shunt} [Ωcm^2]
Industrial 65Ω/sq	200/65	630	36.8	0.793	18.35	1.06	0.53	4707
	120/65	630	37.3	0.789	18.52	1.03	0.69	5097
	80/50	630	37.7	0.767	18.21	1.02	1.10	5013
Low J_{0e} 75Ω/sq	200/65	637	37.0	0.791	18.63	1.07	0.62	4222
	120/65	639	37.6	0.788	18.90	1.05	0.72	5359
	80/50	637	37.8	0.771	18.58	1.05	1.05	6665
Low J_{0e} 55Ω/sq	200/65	635	36.6	0.798	18.53	1.07	0.49	5511
	120/65	635	37.2	0.790	18.64	1.05	0.68	4762
	80/50	635	37.6	0.784	18.73	1.03	0.81	4968

Table 2. Average light *I-V* characteristics of 239cm^2 solar cells fabricated on industrial and low-J_{0e} emitters.

low-J_{0e} 55Ω/sq emitter show a 5mV V_{oc} gain over cells made with the industrial 65Ω/sq emitter. This gain, combined with the higher *FF* that can be achieved because of a lower sheet resistance, enabled an average efficiency of 18.73% and a best efficiency of 18.89% to be realised using only 80mg Ag paste dry mass.

Impact of Ag reduction combined with higher efficiency on manufacturing and system cost

Given the extreme pressure on cell manufacturer profit margins these days, the cost of Ag consumption becomes a key figure of merit, provided cell efficiency remains comparable. Fig. 3 illustrates the US¢/W cost of Ag consumption for each emitter and Ag paste dry mass combination studied. Ag cost values are calculated from cell power output based on data in Table 2, US$32/troy oz Ag market price, and 85% by weight thick-film paste Ag metal content. Additional factors considered in the Ag cost calculation are 2% waste during cell manufacture and 90% cell yield. By comparing the Ag costs for 200 and 120mg Ag paste dry masses, it is seen that solar cells with a low-J_{0e} 75Ω/sq emitter show a slight advantage owing to the higher power output. However, the advantage shifts to solar cells with a low-J_{0e} 55Ω/sq emitter when 80mg Ag paste dry mass is used. Ag cost drops from US¢3.13/W for the 75Ω/sq emitter with 120mg Ag paste dry mass, to US¢2.11/W for the 55Ω/sq emitter with 80mg Ag paste dry mass.

Ag market price volatility was illustrated in the introductory section of this paper. With potential Ag prices ranging from US$4/troy oz to US$50/troy oz, Table 3 explores the impact of Ag market price on the cost of Ag for manufacturing solar cells with a low-J_{0e} 55Ω/sq emitter + 80mg Ag paste dry mass (η_{avg} = 18.73%), as well as for cells with an industrial 65Ω/sq emitter + 120mg Ag paste dry mass (η_{avg} = 18.52%). In the case of a 500mW production line, yearly Ag cost for cells made with a low-J_{0e} 55Ω/sq emitter + 80mg Ag paste dry mass range from US$2.8M to US$15.5M

Ag market price [US$/troy oz]	Ag cost: low J_{0e} 55Ω/sq + 80mg [$M]	Ag cost: industrial 65Ω/sq + 120mg [$M]	Ag cost savings/yr* [$M]
4	2.8	4.2	1.4
10	4.4	6.7	2.2
25	8.6	13.0	4.4
32	10.5	15.9	5.4
50	15.5	23.5	8.0

* $cost_{(industrial\ 65\Omega/sq + 120mg)} - cost_{(low\ J0e\ 55\Omega/sq + 80mg)}$

Table 3. Potential cost savings per year for a 500MW production line at various Ag market prices.

within the market price range given. At US$32/troy oz, the cost advantage for cells made with a low-J_{0e} 55Ω/sq emitter + 80mg Ag paste dry mass translates to a saving of US$5.4M per year over cells made with state-of-the-art industrial 65Ω/sq + 120mg Ag paste dry mass – in other words, a saving of ~33%. Comparison of Ag cost for these two emitter/paste mass combinations is appropriate, since the current industry state of the art is 120mg Ag paste dry mass on high [$P_{surface}$] emitters.

The cost analysis can be extended by observing the impact of the combined Ag reduction and cell efficiency gains observed here on system cost. For this analysis, the industry state-of-the-art cells (η_{avg} = 18.52% with 120mg Ag paste dry mass) and the low-J_{0e} 55Ω/sq cells (η_{avg} = 18.73% with 80mg Ag paste dry mass) are compared. First, average cell efficiencies are converted to module efficiency and corresponding module power. Since one module (area = 1.635m^2) is fabricated from sixty 239cm^2 cells, and the Cz wafers used are pseudo-square, the ratio of cell to module area is 0.877 (1.434m^2/1.635m^2). With cell to module power loss of 4%, the state-of-the-art module efficiency and power are 15.56% and 254.4W, respectively, and the low-J_{0e} 55Ω/sq module efficiency and power are 15.73% and 257.2W, respectively.

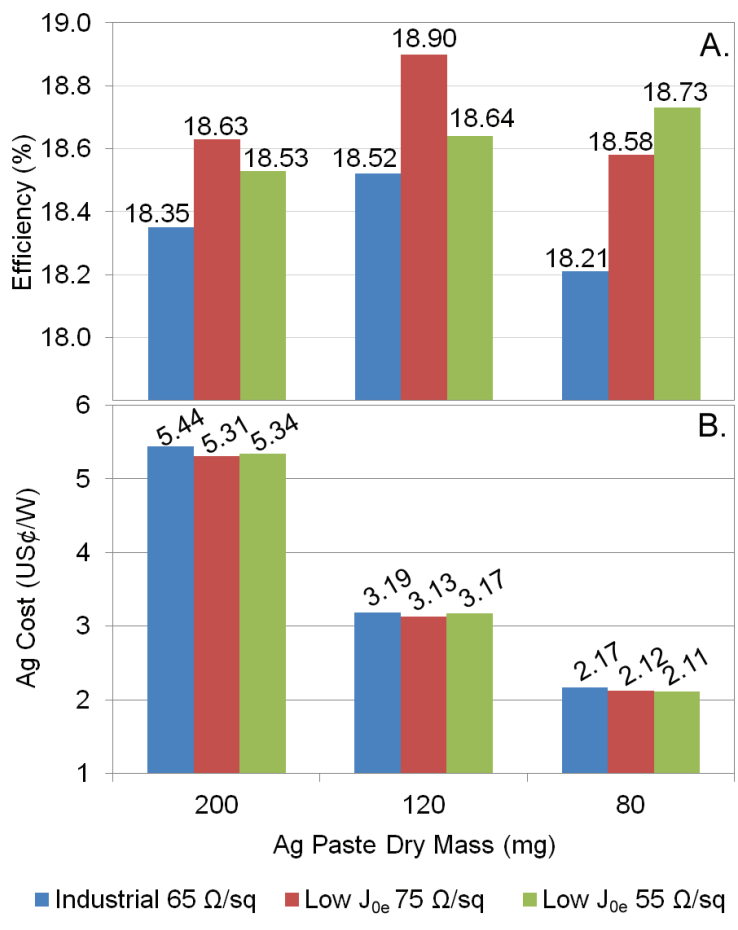

Figure 3. Average efficiency (%) and the cost (US¢/W) for front-side Ag consumption as a function of Ag paste dry mass. Calculation is based on US$32/troy oz Ag market price, 85% by weight paste Ag content, and additional factors.

The 0.2% absolute efficiency improvement observed for modules with cells having the low-J_{0e} 55Ω/sq emitter + 80mg Ag paste dry mass combination will lead to a reduction in area-related BOS costs since fewer modules will be needed for a common power output. (Area-related BOS takes into account installation labour, mounting hardware, support structures, interconnections, wiring and land required during PV system installation.) In general, the higher efficiencies achieved with low-J_{0e} 55Ω/sq modules results in area-related BOS costs that are 1.2% lower, representing a saving of US¢1.10/W [20].

> "As the Ag market price changes, the required additional state-of-the-art module efficiency also changes."

To quantify the impact of Ag reduction, it is possible to calculate the additional absolute module efficiency required for a state-of-the-art module to compensate the Ag cost savings that are realized by using a low-J_{0e} 55Ω/sq module [20]. The effect of Ag cost reduction is decoupled by assuming equal module power for the two compared technologies, and determining the additional module efficiency needed to cancel the Ag cost savings. Assuming a module price of US$0.70/W, in order to maintain the same module manufacturing cost the state-of-the-art module would need a 0.25% absolute higher efficiency to compete with the Ag cost savings afforded by low-J_{0e} 55Ω/sq modules at the US$32/troy oz Ag market price. Fig. 4 shows that, as the Ag market price changes, the required additional state-of-the-art module efficiency also changes. It is interesting to note that, at US$50/troy oz Ag market price, an absolute efficiency enhancement of up to 0.4% would be required for state-of-the-art modules to equal the cost of low-J_{0e} 55Ω/sq modules. The results of this analysis, combined with the 0.2% absolute efficiency gain afforded by low-J_{0e} 55Ω/sq modules, indicates that state-of-the-art modules would require a 0.5% absolute higher efficiency in order to compensate these gains and for both module types to be equal in price.

> "By optimizing emitter diffusion conditions, it was possible to reduce screen-printed Ag paste consumption by 33%, with no loss in cell performance."

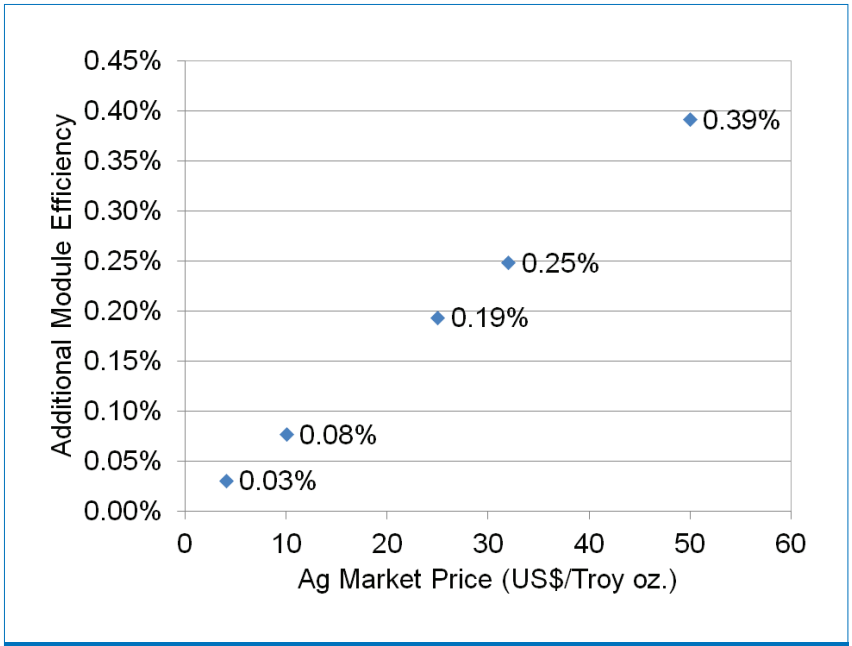

Figure 4. Additional state-of-the-art module efficiency required to offset low-J_{0e} 55Ω/sq module Ag cost savings as a function of Ag market price.

Summary

In order to address the issue of reducing the cost of Ag usage at the same time as maintaining high cell efficiency, phosphorus emitter profiles were tailored via $POCl_3$ diffusion to create solar cell emitters displaying low J_{0e} and low [$P_{surface}$] while minimizing sheet resistance with the aim of reducing Ag consumption. By optimizing emitter diffusion conditions, it was possible to reduce screen-printed Ag paste consumption by 33%, with no loss in cell performance. A screen-printable Ag conductor paste designed to contact low [$P_{surface}$] emitters was used, and the performance of cells with screen-printed Ag paste dry masses of 200, 120 and 80mg was compared. By using tailored low-J_{0e} 55Ω/sq emitters, higher values of V_{oc} and J_{sc} were able to maintain or increase average efficiencies to 18.64% and 18.73% for cells with 80mg and 120mg Ag paste dry weight, respectively. In comparison, an average efficiency of 18.52% was achievable for cells made using state-of-the-art technology (industrial high [$P_{surface}$] emitter with 120mg Ag paste dry mass). On the basis of a Ag market price of USD$32/troy oz and thick-film paste Ag metal content of 85%, a Ag front-side metallization cost of US¢2.11/W can be realized by using 80mg Ag paste dry mass. This figure represents cost savings of 33% and 60%, respectively when compared with Ag costs of US¢3.19/W and US¢5.44/W for traditional, industrial-type emitters using 120–200mg Ag paste dry mass. Further analysis shows that area-related BOS costs for low-J_{0e} 55Ω/sq modules will be 1.2% lower (owing to higher power output) than for state-of-the-art modules. Calculations show that an absolute module efficiency of 0.25% is required for state-of-the-art modules to offset the Ag cost reduction afforded by low-J_{0e} 55Ω/sq modules at current Ag market prices. Finally, in order for state-of-the-art technology to compensate the combination of 0.2% absolute efficiency gain and Ag cost reduction afforded by the low-J_{0e} 55Ω/sq technology, an absolute efficiency enhancement of 0.5% would be required.

References

[1] US Department of Energy 2012, "SunShot vision study" [available online at http://www1.eere.energy.gov/solar/sunshot/vision_study.html].

[2] Silver Price, "Silver price history" [available online at http://silverprice.org/silver-price-history.html].

[3] The Silver Institute, "Silver price history" [available online at http://www.silverinstitute.org/site/silver-price/silver-price-history/].

[4] International Technology Roadmap for Photovoltaics (ITRPV) Results 2011 [available online at http://www.itrpv.net/Reports/].

[5] Lenio, M. et al. 2011, "Design, fabrication and analysis of high efficiency inkjet printed passivated emitter rear contacted cells", *Proc. 37th IEEE PVSC*, Seattle, Washington, USA.

[6] Kray, D. et al. 2011, "Reducing Ag cost and increasing efficiency: Multicrystalline silicon solar cells with direct plated contacts exceeding 17% efficiency", *Proc. 26th EU PVSEC*, Hamburg, Germany.

[7] Bartsch, J. et al. 2010, "Copper as conducting layer in advanced front side metallization processes for crystalline silicon solar cells, exceeding 20% on printed seed layers", *Proc. 35th IEEE PVSC*, Honolulu, Hawaii, USA.

[8] Schulz-Wittmann, O. et al. 2012, "Fine line Cu based metallization for high efficiency solar cells", *Proc. 27th EU PVSEC*, Frankfurt, Germany.

[9] Kyeong, D. et al. 2012, "Approaching 20%-efficiency selective-emitter solar cells with copper front contacts on industrial 156 mm CZ silicon wafers", *Proc. 27th EU PVSEC*, Frankfurt, Germany.

[10] J. Bartsch, J. et al. 2012, "Progress with multi-step metallization processes featuring copper as conducting layer at Fraunhofer ISE", *Proc. 27th EU PVSEC*, Frankfurt, Germany.

[11] Hai, H.T. & Koike, K. 2012, "Replacement of silver by copper for electrodes in c-Si solar cells", *Proc. 27th EU PVSEC*, Frankfurt, Germany.

[12] Ortega, P. et al. 2008, "Very low recombination phosphorus emitters for high efficiency crystalline silicon solar cells", *Semicond. Sci. Technol.*, Vol. 23, p. 125032.

[13] Janssens, T. et al. 2009, "Advanced phosphorus emitters for high efficiency Si solar cells", *Proc. 34th IEEE PVSC*, Philadelphia, Pennsylvania, USA.

[14] Tous, L. et al. 2011, "Evaluating contact resistance using epitaxially grown phosphorus emitters", *Proc. 26th EU PVSEC*, Hamburg, Germany.

[15] Cooper, I.B. et al. 2012, "Low resistance screen-printed Ag contacts to $POCl_3$ emitters with low saturation current density for high efficiency Si solar cells", *Proc. 38th IEEE PVSC*, Austin, Texas, USA.

[16] Mikeska, K.R. et al. 2011, "New thick film paste flux for contacting silicon solar cells", *Proc. 26th EU PVSEC*, Hamburg, Germany.

[17] Green, M.A. 1998, *Solar Cells*. University of New South Wales: Kensington, Australia.

[18] Dastgheib-Shirazi, A. et al. 2012, "Effects of process conditions for the n+-emitter formation in crystalline silicon", *Proc. 38th IEEE PVSC*, Austin, Texas, USA.

[19] Basore, P.A. & Clugston, D.A. 1998, "PC1D Version 5.6", University of New South Wales: Sydney, Australia.

[20] Ristow, A.H. 2008, "Numerical modeling of uncertainty and variability in the technology, manufacturing, and economics of crystalline silicon photovoltaics", Ph.D. dissertation, Georgia Institute of Technology, Atlanta, USA.

About the Authors

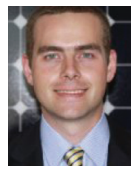

Ian B. Cooper received his Ph.D. degree in physical chemistry from Georgia Tech in 2008. He has been with the University Center of Excellence for Photovoltaics and Education since 2009. His research interests include investigation of low-cost materials and contact metallization for high-efficiency Si solar cells.

Keith Tate studied at Georgia Tech and co-oped with the Georgia Tech Microelectronics Research Center from 1988 until being hired by the University Center of Excellence for Photovoltaics and Education in 1992. He specializes in process development and equipment optimization for front-end device fabrication, along with developing models for device characterization and what-if projections.

Moon Hee Kang is working on his Ph.D. in electrical and computer engineering at Georgia Institute of Technology and has been with the University Center of Excellence for Photovoltaics Research and Education since 2007 as a Graduate Student Assistant. His research focuses on passivation materials and anti-reflective coatings for crystalline silicon solar cells.

Alan Carroll is a Research Fellow at DuPont Microcircuit Materials, where he has worked on the development of DuPont Solamet screen-printable metal contacts for PV cells. He has a Ph.D. in materials engineering science from Virginia Tech.

Kurt Mikeska is a Senior Research Associate with DuPont Central Research, Wilmington, Delaware, and has a Ph.D. in materials science and engineering from Rutgers University. His expertise lies in solid-state inorganic synthesis. He has worked in c-silicon PV for ten years, developing contact metallizations and investigating metal–semiconductor interface contact mechanisms.

Robert Reedy holds a B.S. in electrical engineering from Wayne State University and is a Senior Engineer at the National Renewable Energy Laboratory in Golden, Colorado. He has 20 years' experience in analyzing photovoltaic materials using secondary ion mass spectrometry.

Ajeet Rohatgi received his Ph.D. degree in metallurgy and material science from Lehigh University, Bethlehem, Pennsylvania, in 1977. He is a Regents' and Georgia Power Distinguished Professor in the Georgia Tech School of Electrical and Computer Engineering, the Director of the University Center of Excellence for Photovoltaics and Education, and the Founder/CTO of Suniva, Inc.

Enquiries

Ian B. Cooper
University Center of Excellence for Photovoltaics Research and Education
School of Electrical and Computer Engineering
Georgia Institute of Technology
777 Atlantic Drive NW
Atlanta
Georgia 30332-0250
USA
Tel: 1 (404) 894-4041
Email: ian.cooper@gatech.edu

an event of
THE INNOVATION CLOUD

*more

SOLAREXPO

solarexpo.com

A MUCH *more SPECIALISED EVENT:
PV - CSP - SOLAR THERMAL - SOLAR ARCHITECTURE

A MUCH *more
INTERNATIONAL EVENT

A MUCH *more
STRATEGICALLY CONNECTED EVENT

more than just an expo!

FOUNDING MEMBER
GLOBAL SOLAR ALLIANCE

INTERNATIONAL EXHIBITION AND CONFERENCE - 14th edition

MILAN • 8 - 10 MAY 2013